Multilevel DC–DC Power Conversion System With Multiple DC Sources

Miaosen Shen, *Member, IEEE*, Fang Zheng Peng, *Fellow, IEEE*, and Leon M. Tolbert, *Senior Member, IEEE*

***Abstract*—A multilevel dc–dc power conversion system with multiple dc sources is proposed in this paper. With this conversion system, the output voltage can be changed almost continuously without any magnetic components. With this magnetic-less system, very high temperature operation is possible. Power loss and efficiency analysis is provided in the paper. Comparison results show that the system does not require more semiconductors or capacitance than the traditional boost converter. Experimental results are provided to confirm the analysis and control concept.**

***Index Terms*—DC–DC power conversion, multilevel converter, pulsewidth modulation (PWM).**

I. Introduction

TRADITIONAL dc–dc converters require at least one inductive component, which is bulky, heavy, and costly. With the technology advancement of the silicon carbide (SiC) devices and ceramic capacitors, very high temperature components (above 250 °C) will be available except magnetic cores. Thus, very high temperature operation of magnetic-less converter becomes possible and very attractive because natural air cooling can be adopted, which will reduce the size, weight, and the cost of the converter significantly. The multilevel dc–dc converter [1]–[15] becomes a good candidate for this application, because there are no magnetic components necessary, and also because of its bidirectional nature. Traditional multilevel dc–dc converters usually output a fixed voltage for a given input voltage, this may become a drawback of these converters because for some applications, such as hybrid vehicles, a variable dc bus voltage is preferable so that the inverter can always be operated at its most efficient dc voltage. In this paper, a bidirectional multilevel dc–dc conversion system that can output variable voltage with multiple dc sources will be proposed.

II. Description of the DC–DC Conversion System

The proposed dc–dc conversion system is shown in Fig. 1(a), where there are n isolated dc sources, $V_{dc1} \sim V_{dcn}$, and n identical dc–dc converters cells with the output connected in series.

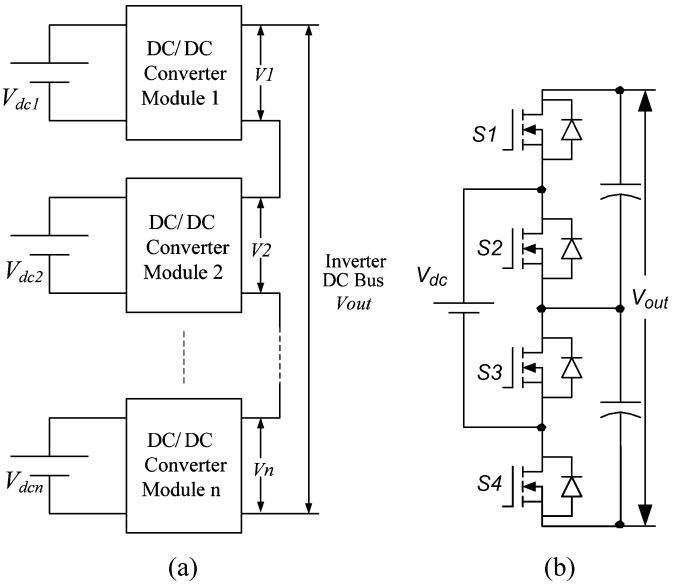

Fig. 1. DC–DC power conversion system configuration and converter cell topology: (a) dc–dc power converter system configuration and (b) topology of the dc–dc converter module.

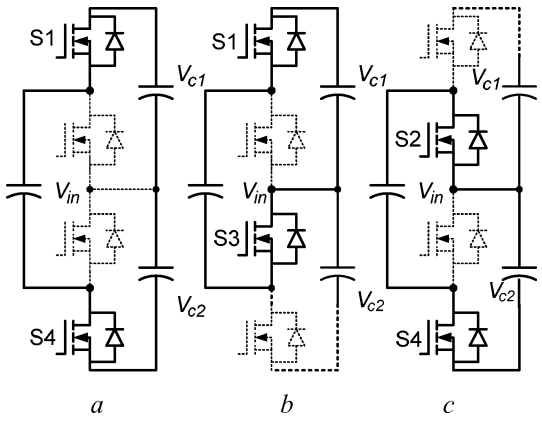

Fig. 2. Converter switching states.

One possible application of this topology is hybrid electric vehicles, instead of connecting all batteries in series as one power source and a bidirectional boost converter to interface the battery and the dc bus, one can use separate batteries to power separate converter modules and connect the output of the modules in series as a dc bus supplying the inverter. The dc–dc converter cell is shown in Fig. 1(b), which is a two level converter.

For each dc–dc converter cell as shown in Fig. 1(b), there are three switching states as illustrated in Fig. 2.

Manuscript received April 16, 2007; revised June 21, 2007. Recommended for publication by Associate Editor B. Wu.

M. Shen is with Siemens VDO Electric Drives, Inc., Dearborn, MI 48120 USA (e-mail: miaosen.shen@siemens.com).

F. Z. Peng is with the Department of Electrical and Computer Engineering, Michigan State University, Lansing, MI 48824 USA (e-mail: fzpeng@egr.msu.edu).

L. M. Tolbert is with The University of Tennessee, Knoxville, TN 37996-2100 USA (e-mail: tolbert@utk.edu).

Color versions of one or more of the figures in this paper are available online at http://ieeexplore.ieee.org.

Digital Object Identifier 10.1109/TPEL.2007.911875

With these three switching states, the converter is able to output two different voltages. When the converter is in switching state a, (switches S1 and S4 are on, S2 and S3 are off), the following equation will be met

$$V_{\text{out}} = V_{\text{in}}. \tag{1}$$

Obviously, when the switches (MOSFETs or IGBTs with free wheeling diodes) are turned on, the current can flow in either direction, so the converter is a bidirectional converter.

In the second mode, the converter alternates its switching states between b and c complementarily with 50% duty ratio for each switching state at a high frequency, the following equations will be met

$$V_{c1} = V_{\text{in}}, \quad V_{c2} = V_{\text{in}}. \tag{2}$$

Thus, the output voltage is $V_{\text{out}} = 2V_{\text{in}}$. Also, the converter is bidirectional in this mode.

Therefore, each single module is able to output two different voltages: V_{in} or $2V_{\text{in}}$. For a system that consists of n cells, the system is able to output $n+1$ different voltages from nV_{in} to $2nV_{\text{in}}$ with step of V_{in}. When the number of n increases, the output voltage can be considered as almost continuous, and the inverter fed by the dc–dc converter can always operate close to the optimum voltage point.

III. Converter Control During Transition

In steady state, the voltage difference between the battery and the capacitors being charged/discharged is very small, therefore the current through the switches is well limited. During transition when one wants to change the output voltage between V_{in} and $2V_{\text{in}}$, the voltage difference between the two could be relatively large, which might result in high transient current. To limit the current, a small inductor as shown in Fig. 3 is considered, the requirement of the inductance is very small (<1 μH), and as will be shown in a later section, it can be considered as the parasitic inductance of the cable and the equivalent series inductance (ESL) of the capacitor on the battery side. Usually the parasitic inductance would be large enough especially for hybrid electric vehicles if the battery is not placed adjacent to the converter.

A. Change the Output Voltage From V_{in} to $2V_{\text{in}}$

Before the output voltage is changed to $2V_{\text{in}}$, the capacitor voltage, V_c, equals to half of the battery voltage. In this transition, the two capacitors will be charged up from half input voltage to full input voltage, thus input current will be higher when the battery is outputting power during the transition compared with when charging the battery. Therefore, the battery is assumed to be outputting current during the transition as the condition is more critical. When the transition starts, the converter starts to get into switching states b and c, and the equivalent circuits when charging C1 and C2 are shown in Fig. 4(a) and (b), respectively.

In the transition, the battery is charging the two capacitors equally. Fig. 4(a) and (b) each shows half of the operation condition. In each condition, there are two switching states: the switch (S2 or S3) is on or the switch is off. When the switch is on, V_i equals to one capacitor voltage; when it is off, it equals to the sum of the two capacitor voltages because of the freewheeling. Thus the effect the switching state when S2 is turned on is the same as the state when S3 is turned on in terms of inductor current. Defining the duty ratio, D, as the sum of the duty ratio of S3 and S2 and assuming that the inductor current is in continuous mode, in steady state, the relationship of the capacitor voltage and the input voltage is

$$V_{\text{in}} = \overline{V}_i = DV_c + (1-D) \times 2V_c = (2-D)V_c. \tag{3}$$

From above equation, the duty ratio should be gradually increased from 0 to 1 in order to increase the capacitor voltage from $V_{\text{in}}/2$ to V_{in} gradually. As a result, the switching signals shown in Fig. 5 are required to control the switches. S2 and S3 show the actual duty cycle, which is half of D, S1 and S4 are inverted signals of S2 and S3, respectively.

B. Change the Output Voltage From 2 V_{in} to 1 V_{in}

Before changing the output voltage from $2V_{\text{in}}$ to V_{in}, the capacitor voltage equals to battery voltage. The capacitor voltage will be discharged from the battery voltage to half of it, thus the transition is more critical when the battery is being charged by

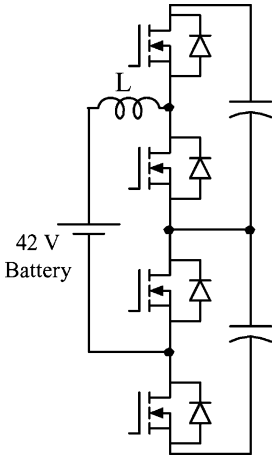

Fig. 3. Converter with small inductance.

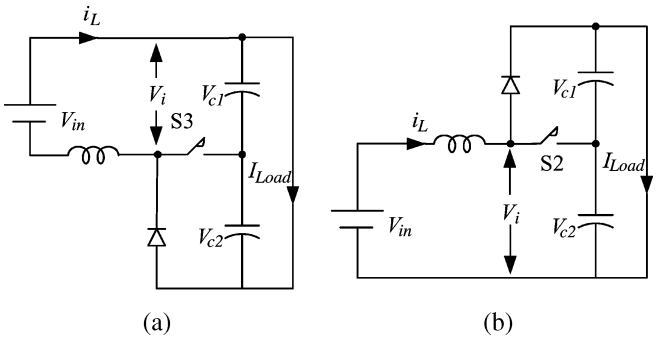

Fig. 4. Equivalent circuit of switching states (b) and (c).

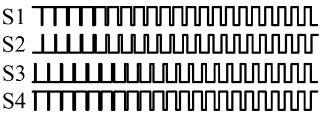

Fig. 5. Control signals during output voltage transient from V_{in} to $2V_{\text{in}}$.

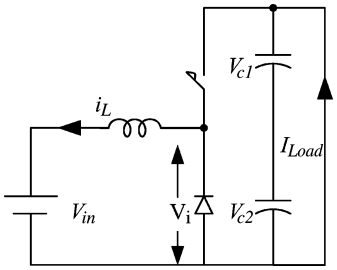

Fig. 6. Equivalent circuit for switching state (a).

Fig. 7. Control signals during output voltage transient from $2V_{\rm in}$ to $V_{\rm in}$.

the load. The equivalent circuit of switching state a is shown in Fig. 6. When the switch is turned on, S1 and S4 are turned on in the actual circuit. When these two switches are on, V_i equals to twice of the capacitor voltage, otherwise V_i equals to zero due to freewheeling. Assuming the duty ratio is D, the relationship of the voltages and the duty ratio for continuous current condition is

$$V_{\rm in} = 2DV_c. \tag{4}$$

As a result, the duty ratio should change from 0.5 to 1 gradually to control the capacitor voltage from $V_{\rm in}$ to $V_{\rm in}/2$ as shown in Fig. 7. S2 and S3 are inverted signals of S1 and S4.

When the switching frequency is relatively low, using the above method may not be sufficient to limit the peak current because the current change in one cycle can be relatively big due to small inductance. To further suppress the peak current during transient, a higher switching frequency may be used during the transition.

IV. Output Voltage Loss

When outputting $2*\mathrm{Vin}$, dead time has to be implemented in order to prevent shoot through. Assume that the input current is continuous because of the small parasitic inductor, and the duty cycle is D (the percentage of time the input is connected to either of the capacitors). When the input is connected to one of the capacitors, the voltage across the parasitic inductor is

$$V_L = V_{\rm in} - V_c. \tag{5}$$

During the dead time, if the battery is outputting power to the load, the current flows through the freewheeling diodes of S1 and S4 to charge both capacitors, and the voltage across the inductor is

$$V_L = V_{\rm in} - 2V_c. \tag{6}$$

If the battery is being charged from the load side, the current flows through the freewheeling diodes of S2 and S3, and the voltage across the inductor is

$$V_L = V_{\rm in}. \tag{7}$$

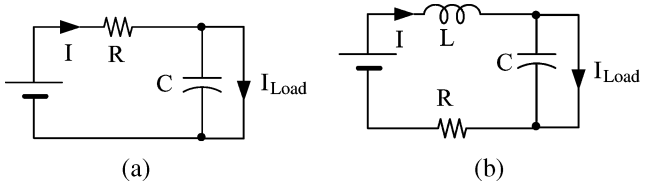

Fig. 8. Equivalent circuit with and without the parasitic inductance.

Thus, the steady state output voltage depends on the direction of the power flow. When the battery is powering the load, the output voltage is

$$V_{\rm out} = \frac{2V_{\rm in}}{2-D}. \tag{8}$$

The output voltage when the battery is being charged by the load is

$$V_{\rm out} = \frac{2V_{\rm in}}{D}. \tag{9}$$

Thus, the output voltage could be slightly different depending on the power flow direction and dead time. Also the voltage drop across the switches should be included.

V. Power Loss Analysis

In previous literature [1]–[3], the power loss of this type of converter is analyzed. In the literature, the parasitic inductance is not considered, and the RC constant of the converter is always comparable to the switching period to achieve high efficiency. When considering the small parasitic inductance, results differ. When the input is connected to one of the capacitors, the equivalent circuits with and without considering the parasitic inductor are shown in Fig. 8(a), where $I_{\rm Load}$ is the load current. When there is no inductance, the current can be expressed by the following equation:

$$i(t) = \frac{V_0}{R}e^{-\frac{t}{RC}} + I_{\rm Load} \tag{10}$$

where V_0 is the initial voltage difference between the voltage source and the voltage across the capacitor. The current waveform is shown in Fig. 9, the shaded area corresponds to the average input current.

When considering the parasitic inductor, the input current is

$$\begin{aligned} i(t) &= I_{\rm Load} + I_0 e^{-\frac{R}{2L}t}\cos\left(\sqrt{\frac{1}{LC}+\left(\frac{R}{2L}\right)^2}\,t\right) \\ &\quad + \frac{V_0 - \frac{RI_0}{2}}{\sqrt{\frac{L}{C}-\left(\frac{R}{2}\right)^2}}e^{-\frac{R}{2L}t}\sin\left(\sqrt{\frac{1}{LC}-\left(\frac{R}{2L}\right)^2}\,t\right) \\ &= I_{\rm Load} + f(I_0,V_0)e^{-\frac{R}{2L}t} \\ &\quad \times \sin\left(\sqrt{\frac{1}{LC}-\left(\frac{R}{2L}\right)^2}\,t + \varphi(I_0,V_0)\right) \end{aligned} \tag{11}$$

where $I_{\rm Load}+I_0$ and V_0 are the initial current and initial voltage difference between the input voltage and capacitor. Another feature of this case is that the initial current and the current when the switch turns off are the same because the converter repeats the same process with the other capacitor after it finishes charging

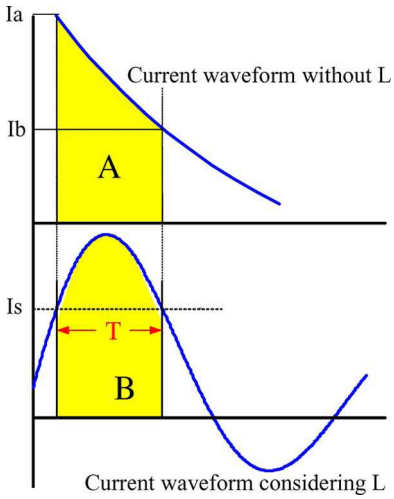

Fig. 9. Input current of the converter with and without parasitic inductance.

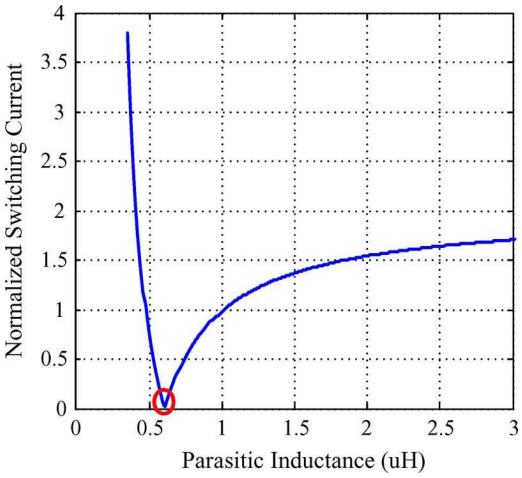

Fig. 11. Normalized switching current versus L.

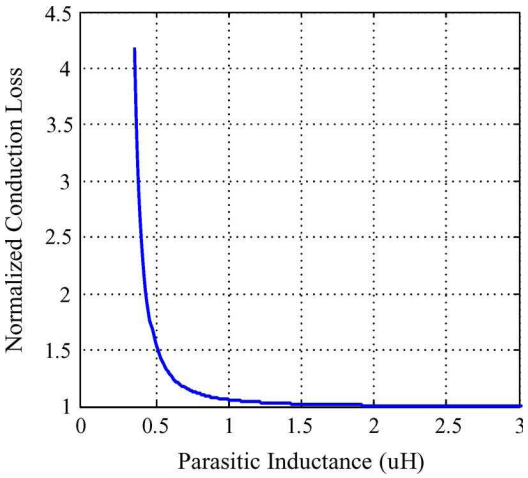

Fig. 10. Normalized conduction loss versus L.

one capacitor. Thus the input current is shown in Fig. 9 with the initial current equal to the current at the end of the process, the shaded area corresponds to the average input current.

For a fixed output power and given input voltage, the average input current is fixed (area A should equal to area B for the same power and voltage), different inductance results in different input current shape, which further results in different input current rms value. The conduction loss of the circuit is directly proportional to the square of the rms value assuming MOSFETs are used as the switches. Based on the above equations, one can easily numerically calculate the ratio of rms current over the average current based on the different parameters, and from which the loss can be calculated. As an example, Fig. 10 shows the normalized conduction loss of a converter with different parasitic inductances, the other parameters of the converter are: $R_{\rm ds}$on (MOSFET on resistance) $=$ 1 mΩ, C (capacitance of each capacitor) $=$ 1 mF, f_s (switching frequency) $=$ 5 kHz. The normalized loss with no parasitic inductance is 7.0. From which we can see that the conduction loss is dramatically reduced with a small parasitic inductance.

The switching loss is directly proportional to the switching current given the fixed converter voltage. It is noteworthy that half of the switching actions in this converter is zero voltage switching due to the current freewheeling through the body diodes during the dead time. The switching current is the initial and ending current, I_a, I_b, and I_s, shown in Fig. 9. Fig. 11 shows the switching current normalized by the average current for the same converter versus different parasitic inductances. From Fig. 11, the switching current reduces as the parasitic inductance reduces until it reaches the resonant point with 0.6 μH and then increases again with further reducing of the inductance. The normalized switching current of the system without any parasitic inductance is 26.

With small amount of parasitic inductance, both conduction loss and switching loss are reduced significantly compared to the system with zero inductance. In previous literature [1]–[3], the capacitance has to be relatively large so that the time constant of RC is comparable to switching period to keep high efficiency. In other words, the converter's capacitance requirement is dramatically reduced with small parasitic inductance.

VI. Cost Comparison With Other Topologies

The proposed topology is an alternative to the traditional boost converter and traditional switched capacitor converter shown in Fig. 12. The switched capacitor converter can be improved by adding an inductor in series with C_{s1} and operating the converter as a resonant converter [10]. To compare the cost of the converter with the traditional bidirectional boost converter and traditional switched capacitor converters, the semiconductor VA rating and the capacitor current capability, voltage rating, and capacitance requirement are compared. Define the semiconductor VA rating as the product of the average current that flows through the device and the maximum voltage across it. For a traditional bidirectional boost converter, the sum of the VA rating of the two switches is

$$VA_{\rm traditional} = V_{\rm out} * I_{\rm in} \tag{12}$$

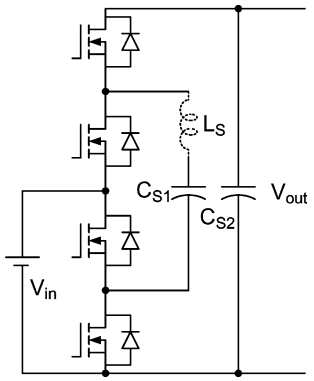

Fig. 12. Traditional switched capacitor two-level converter.

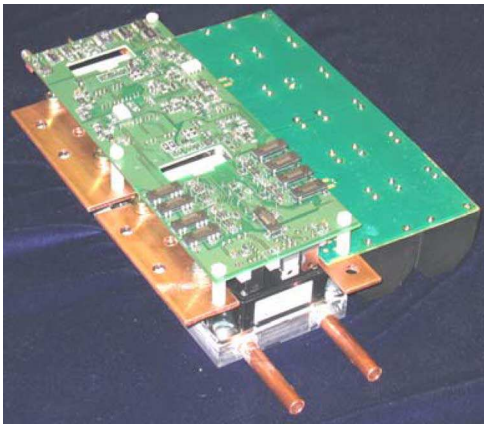

Fig. 13. DC–DC converter module.

where $V_{\rm out}$ is the output voltage and $I_{\rm in}$ is the input average current.

For the proposed converter and the traditional switched capacitor converter [10]–[15], there are four switches and each of them sustains half of the output voltage and conveys the input current during half of the time, thus the total VA rating is

$$VA_{\rm proposed} = VA_{\rm switchedcapacitor} = 4 * \frac{V_{\rm out}}{2} * \frac{I_{\rm in}}{2} = V_{\rm out} * I_{\rm in}. \tag{13}$$

Therefore, the total VA ratings of the semiconductors are the same for all three topologies.

To compare the capacitor requirement, the traditional boost converter is assumed to be operated with duty ratio of 50%, so that the boost ratio is the same as the proposed converter. For traditional boost converter, the capacitor current is square wave and with an rms value of half of the input current assuming that the input current is constant. The capacitor has to sustain full output voltage. The capacitance is determined by the allowable output voltage ripple. For the boost converter, the capacitance requirement can be calculated by

$$C_{\rm boost} = \frac{I_{\rm in}}{4 f_s \Delta V} \tag{14}$$

where f_s is the switching frequency and ΔV is the allowable output voltage ripple.

For traditional switched capacitor without any inductor, the capacitor current is similar to the proposed converter without any inductor, so the rms current can be very high. For the case with a small inductor and a circuit that operates as a resonant converter [10], the rms current through C_{s1} equals to the input current. It is noteworthy that the inductor current is sinusoidal, thus the rms current is 1.11 times of the boost converter case, which is square waveform. The voltage across C_{s1} equals to the input voltage. The capacitance of C_{s1} does not have to be high as long as the voltage ripple is reasonable. The operation condition of $Cs2$ is very similar to the output capacitor of boost converter with slightly higher current rating because of the input current to the capacitor is sinusoidal instead of square waveform. The voltage rating and capacitance should be the same.

For the proposed converter, the two capacitor current ratings are the same as that in the boost converter, $I_{\rm in}/2$, assuming that the input current is close to constant. Each of the capacitors sustains only half of the output voltage. In this topology, one of the capacitors is being charged while the other is being discharged, therefore the output voltage ripple is much smaller than the traditional boost converter for the same capacitance because of the cancellation of the ripple across each capacitor. This results in much lower capacitance requirement than the traditional boost converter for the same output voltage ripple requirement.

In short, the proposed converter requires minimum capacitive components. The boost converter requires similar or higher capacitive components depending on which parameter defines the capacitor size. The switched capacitor converter needs the most capacitors.

The boost converter needs a fairly large inductor to operate properly. The traditional switched capacitor converter needs a small inductor with relatively precise inductance to operate in resonant mode. The proposed converter only needs very small inductance to operate in high efficiency mode, and the inductance can be the stray inductance of the cables or an air core inductor if the stray inductance is not enough.

VII. Experimental Results

To verify the concept, a 10 kW dc–dc converter shown in Fig. 13 has been built. The switches used are MOSFET module FM600TU-07A, 1 mF film capacitors are used for both capacitors C1 and C2. The converter operates at 5 kHz for steady state operation when outputting 2 Vin, and it operates at 50 kHz during the 15-ms transition between 1 Vin to 2 Vin to limit the transient current. No extra inductor is used and the battery is connected to the converter from 30 cm away.

Fig. 14(a) shows the input and output current/voltage when outputting 1 $V_{\rm in}$. Fig. 14(b) shows the same waveforms when outputting 2 $V_{\rm in}$. As can be seen from Fig. 14, the input current is continuous and has exactly the same shape as depicted in Fig. 9. Also, it is noteworthy that the output voltage does not quite reach twice of the input voltage, which is caused by the voltage loss across the switches and dead time. Fig. 14(c) and (d) shows the transition between 1 $V_{\rm in}$ and 2 $V_{\rm in}$. As can be seen from the results, the current is well regulated during steady state operation and well limited during the transition. The transition time is only 15 ms.

The converter efficiency is measured at different input voltages and different powers as shown in Fig. 15. As can be seen from the figure, the efficiency is quite high. The reduction of the efficiency at low power is mainly because of the control and

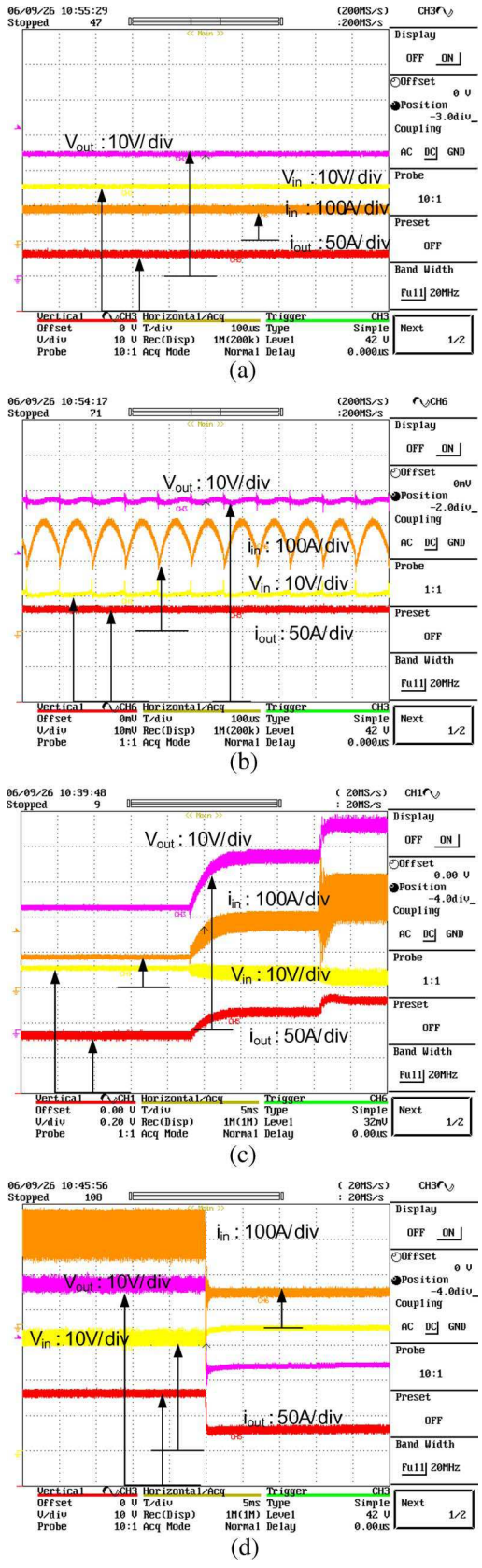

Fig. 14. Experimental results of the converter, 1 Vin means the output voltage equals to input voltage, 2 Vin means the output voltage is twice of the input voltage. (a) Steady state waveform when outputting 1 Vin; (b) steady state waveform when outputting 2 Vin; (c) transition from 1 Vin to 2 Vin; (d) transition from 2 Vin to 1 Vin.

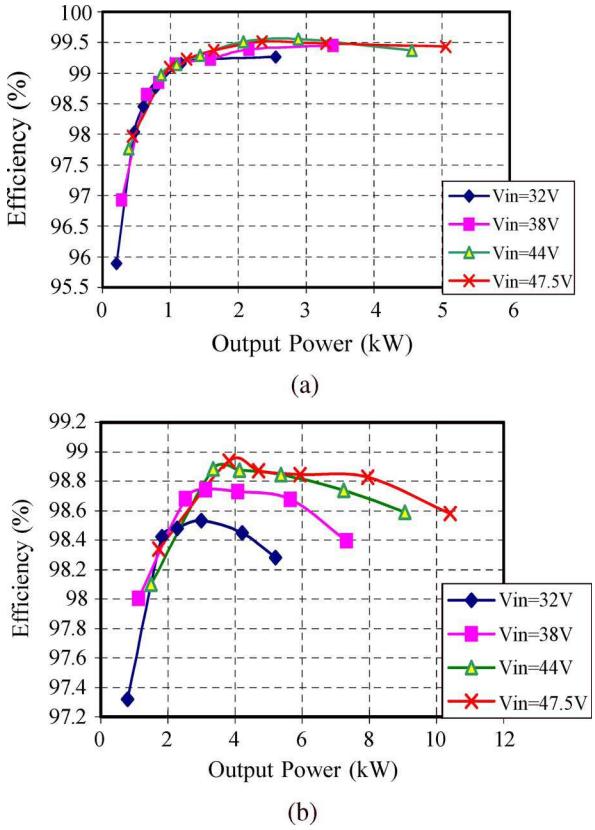

Fig. 15. Measured efficiency of multilevel dc–dc converter: (a) when outputting 1 Vin and (b) when outputting 2 Vin.

gate drive power becomes significant in terms of percentage at low power.

Compared to the switched capacitor converter without any inductor, the proposed converter offers much higher efficiency given the same circuit parameters as discussed above. For the resonant switched capacitor converter, the switching loss is zero and the current through the capacitor is sinusoidal if the circuit operates exactly at the resonant point. However, if the inductance value is off from the value required for resonance, both switching loss and conduction loss will increase significantly. The proposed converter can achieve the resonant point with zero switching loss with proper inductance as shown in Fig. 11. At the resonant point, the current through the switches are of the same shape and therefore should have the same efficiency as the resonant switched capacitor converter. However, unlike the resonant switched capacitor converter, when the inductance is larger than the resonant value, the conduction loss reduces while the switching loss increases. Therefore, the proposed converter is able to offer the same efficiency as the resonant switched capacitor converter if the resonant point is perfectly achieved; the proposed converter will deliver higher efficiency if the inductance is higher than the desired inductance.

VIII. Conclusion

In this paper, a multilevel dc–dc conversion system with multiple dc sources is proposed. Circuit analysis and control are presented. Analysis shows that a small amount of parasitic inductance reduces the power loss in the converter dramatically and reduces the capacitance requirement significantly. Also,

it was shown that the requirement of semiconductor of the proposed multilevel converter is no greater than the traditional boost converter and switched capacitor converters and that the proposed converter requires less capacitance. Experimental results are provided to confirm the functionality without any extra inductors. With the help of parasitic inductance of the connection cable, the current during transition is well regulated. The requirement of the parasitic inductance can be further reduced by increasing the switching frequency during transition time. In case the stray inductance is not sufficiently large, a small air core inductor can be used. The high efficiency nature is proved by experimental results. This topology provides the potential for high temperature operation of dc–dc converters.

ACKNOWLEDGMENT

The authors would like to thank Dr. H. Xu and Ms. W. Qian for their help in measuring the converter efficiency.

REFERENCES

[1] Z. Pan, F. Zhang, and F. Z. Peng, "Power losses and efficiency analysis of multilevel DC-DC converters," in *Proc. IEEE Appl. Power Electron. Conf.*, Mar. 2005, pp. 1393–1398.

[2] F. Zhang, F. Z. Peng, and Z. Qian, "Study of multilevel converters in DC-DC application," in *Proc. IEEE Power Electron. Spec. Conf.*, Jun. 2004, pp. 1702–1706.

[3] F. Z. Peng, F. Zhang, and Z. Qian, "A novel compact DC-DC converter for 42 V systems," in *Proc. IEEE Power Electron. Spec. Conf.*, Jun. 2003, pp. 33–38.

[4] K. D. T. Ngo and R. Webster, "Steady-state analysis and design of a switched-capacitor DC–DC converter," *IEEE Trans. Aerosp. Electron. Syst.*, vol. 30, no. 1, pp. 92–101, Jan. 1994.

[5] W. Harris and K. Ngo, "Power switched-capacitor DC-DC converter, analysis, and design," *IEEE Trans. Aerosp. Electron. Syst.*, vol. 33, no. 2, pp. 386–395, Apr. 1997.

[6] S. V. Cheong, H. Chung, and A. Ioinovici, "Inductor-less dc-to-dc converter with high power density," *IEEE Trans. Ind. Electron.*, vol. 41, no. 2, pp. 208–215, Apr. 1994.

[7] F. Khan and L. Tolbert, "A multilevel modular capacitor clamped dc–dc converter," in *Proc. IEEE Ind. Appl. Annu. Meeting*, Oct. 2006, pp. 966–973.

[8] F. Zhang, L. Du, F. Z. Peng, and Z. Qian, "A new design method for high efficiency DC-DC converters with flying capacitor technology," in *Proc. IEEE Appl. Power Electron. Conf.*, Mar. 2006, pp. 92–96.

[9] B. Ozpineci, L. M. Tolbert, G.-J. Su, and Z. Du, "Optimum fuel cell utilization with multilevel DC-DC converters," in *Proc. IEEE Appl. Power Electron. Conf.*, Mar. 2004, pp. 1572–1576.

[10] K. K. Law, K. W. E. Cheng, and Y. P. B. Yeung, "Design and analysis of switched-capacitor-based step-up resonant converters," *IEEE Trans. Circuits Syst. I*, vol. 52, no. 5, pp. 943–948, May 2005.

[11] F. L. Luo and H. Ye, "Positive output multiple-lift push-pull switched-capacitor Luo-converter," *IEEE Trans. Ind. Electron.*, vol. 51, no. 3, pp. 594–602, Jun. 2004.

[12] B. R. Gregoire, "A compact switched-capacitor regulated charge pump power supply," *IEEE J. Solid-State Circuits*, vol. 41, no. 8, pp. 1944–1953, Aug. 2006.

[13] J. W. Kimball, P. T. Krein, and K. R. Cahill, "Modeling of capacitor impedance in switching converters," *IEEE Power Electron. Lett.*, vol. 3, no. 4, pp. 136–140, Dec. 2005.

[14] J. Han, A. Jouanne, and G. C. Temes, "A new approach to reducing output ripple in switched-capacitor-based step-down dc-dc converters," *IEEE Trans. Power Electron.*, vol. 21, no. 6, pp. 1548–1555, Nov. 2006.

[15] B. Arntzen and D. Marksimovic, "Switched capacitor dc–dc converters with resonant gate drive," *IEEE Trans. Power Electron.*, vol. 13, no. 5, pp. 892–902, Sep. 1998.

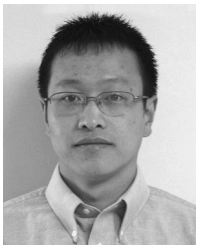

Miaosen Shen (S'04–M'07) received the B.S. and M.S. degrees from Zhejiang University, Hangzhou, China, in 2000 and 2003, respectively, and the Ph.D degree from Michigan State University, East Lansing, in 2007, all in electrical engineering.

Since 2007, he has been with Siemens VDO Electric Drives, Inc., Dearborn, MI, working on hybrid electric vehicles. His research interests include hybrid electric vehicle, dc–dc power conversion, power factor correction technique, and electronic ballast for HID lamps.

Fang Zheng Peng (M'92–SM'96–F'05) received the B.S. degree in electrical engineering from Wuhan University, Wuhan, China, in 1983 and the M.S. and Ph.D. degrees in electrical engineering from Nagaoka University of Technology, Niigata, Japan, in 1987 and 1990, respectively.

He joined Toyo Electric Manufacturing Company, Ltd., where he worked from 1990 to 1992 as a Research Scientist engaged in research and development of active power filters, flexible ac transmission systems (FACTS) applications, and motor drives. From 1992 to 1994, he worked with the Tokyo Institute of Technology as a Research Assistant Professor, where he initiated a multilevel inverter program for FACTS applications and a speed-sensorless vector control project. From 1994 to 2000, he worked for Oak Ridge National Laboratory (ORNL), as a Research Assistant Professor at the University of Tennessee, Knoxville, from 1994 to 1997, and was a staff member, Lead (principal) Scientist of the Power Electronics and Electric Machinery Research Center, ORNL, from 1997 to 2000. In 2000, he joined Michigan State University, Lansing, as an Associate Professor and now a Full Professor of the Department of Electrical and Computer Engineering. He holds over 10 patents.

Dr. Peng received the 1996 First Prize Paper Award and the 1995 Second Prize Paper Award from the Industrial Power Converter Committee, IEEE/IAS Annual Meeting; the 1996 Advanced Technology Award from the Inventors Clubs of America, Inc., the International Hall of Fame; the 1991 First Prize Paper Award in the IEEE TRANSACTIONS ON INDUSTRY APPLICATIONS; and the 1990 Best Paper Award in the Transactions of the IEE of Japan (the Promotion Award of Electrical Academy). He was an Associate Editor for the IEEE TRANSACTIONS ON POWER ELECTRONICS from 1997 to 2001 and has been an Associate Editor again since 2005. He was Chair of Technical Committee for Rectifiers and Inverters of IEEE Power Electronics Society from 2001 to 2005.

Leon M. Tolbert (S'89–M'91–SM'98) received the B.E.E., M.S., and Ph.D. degrees in electrical engineering from the Georgia Institute of Technology, Atlanta, in 1989, 1991, and 1999, respectively.

He joined the Engineering Division of Lockheed Martin Energy Systems in 1991 and worked on several electrical distribution projects at the three U.S. Department of Energy plants in Oak Ridge, TN. In 1997, he became a Research Engineer in the Power Electronics and Electric Machinery Research Center, Oak Ridge National Laboratory (ORNL). Presently, he is an Associate Professor in the Department of Electrical and Computer Engineering, University of Tennessee, Knoxville, where he has worked since 1999. He is also an Adjunct Participant at ORNL and conducts joint research at the National Transportation Research Center (NTRC). He does research in the areas of electric power conversion for distributed energy sources, motor drives, multilevel converters, hybrid electric vehicles, and application of SiC power electronics.

Dr. Tolbert received the 2001 IAS Outstanding Young Member Award. He was an Associate Editor of the IEEE POWER ELECTRONICS LETTERS from 2003 to 2006 and is currently an Associate Editor of the IEEE TRANSACTIONS ON POWER ELECTRONICS. He was Chair of the Education Activities Committee of the IEEE Power Electronics Society from 2003 to 2007. He was the Coordinator of Special Activities for the Industrial Power Converter Committee of IAS from 2003 to 2006. He is a Registered Professional Engineer in the state of Tennessee.